



COMPROMETIDA COM A PROMOÇÃO DO DESENVOLVIMENTO DA ENGENHARIA E DAS CIÊNCIAS MECÂNICAS

VI CONGRESSO NACIONAL DE ENGENHARIA MECÂNICA
VI NATIONAL CONGRESS OF MECHANICAL ENGINEERING
18 a 21 de agosto de 2010 – Campina Grande – Paraíba - Brasil
August 18 – 21, 2010 – Campina Grande – Paraíba – Brazil

QUENCHING ANALYSIS OF NOTCHED STEEL CYLINDERS USING THE FINITE ELEMENT METHOD

Wendell Porto de Oliveira, wendell@furnas.com.br¹
Marcelo Amorim Savi, savi@mecanica.ufrj.br¹
Pedro Manuel Calas Lopes Pacheco, calas@cefet-rj.br²

¹ Universidade Federal do Rio de Janeiro - COPPE – Department of Mechanical Engineering
21.941.972 – Rio de Janeiro – RJ - Brazil, P.O. Box 68.503

² CEFET/RJ - PPEMM - Programa de Pós-Graduação em Engenharia Mecânica e Tecnologia de Materiais
Av. Maracanã, 229, 20271-110 - Rio de Janeiro - RJ – Brazil

***Abstract.** Quenching is a commonly used heat treatment process employed to control the mechanical properties of steels. The resulting microstructures formed from quenching (pearlite, ferrite, bainite and martensite) depend on cooling rate and on steel characteristics. This article deals with the modeling and simulation of quenching using a multi-phase constitutive model. The through hardening is considered as an application of the proposed general formulation. Finite element method is employed for spatial discretization. Notched steel cylinders are of concern evaluating the influence of notches in quenched pieces. Numerical simulations evaluate temperature evolution and phase transformation distribution through the process. Stress distribution is also of concern treating time evolution and residual stresses through the piece.*

***Keywords:** Quenching, Modeling, Finite Element Method, Residual Stresses*

1. INTRODUÇÃO

Heat treatments are usually employed in industrial processes and quenching is one of the most common processes. It provides a mean to control some mechanical properties of steels as tensile strength, toughness and hardness. The phases and constituents formed from quenching results in different microstructures (ferrite, cementite, pearlite, upper bainite, lower bainite and martensite) which depend on cooling rate and on chemical composition of the steel. Phase transformation combined with large temperature gradients and non-uniform cooling can promote high residual stresses in quenched steels.

Phenomenological aspects of quenching involve couplings among different physical processes and its description is unusually complex. Among them, thermal, phase transformation and mechanical are some important phenomena involved. The description of each one of these phenomena has been addressed by several authors by considering these aspects separately. Sen *et al.* (2000) considered steel cylinders without phase transformations. There are also references that focus on the modeling of the phase transformation phenomenon (Hömborg, 1996; Chen *et al.*, 1997, Çetinel *et al.*, 2000; Reti *et al.*, 2001). Several authors have proposed coupled models that are not generic and are usually applicable to simple geometries as cylinders (Inoue & Wang, 1985; Melander, 1985; Sjöström, 1985; Denis *et al.*, 1985, 1987, 1999; Fernandes *et al.*, 1985; Woodard, *et al.*, 1999). Moreover, there are some complex aspects that are usually neglected in the analysis of quenching process. As an example, one could mention the heat generated during phase transformation. This phenomenon is usually treated by means of the latent heat associated with phase transformation (Inoue & Wang, 1985; Denis *et al.*, 1987, 1999; Woodward *et al.*, 1999). Meanwhile, other coupling terms in the energy equation related to other phenomena as plastic strain or hardening are not treated in literature and their analysis is an important topic to be investigated. Silva *et al.* (2004) analyzed the thermomechanical coupling during quenching considering austenite-martensite phase transformations. Silva *et al.* (2005) employed the finite element method to study the phase transformation effect in residual stresses generated by quenching in notched steel cylinders.

This article deals with the modeling and simulation of quenching in steel cylinders using a multi-phase constitutive model with internal variables formulated within the framework of continuum mechanics and the thermodynamics of irreversible processes. A numerical procedure is developed based on the operator split technique associated with an iterative numerical scheme in order to deal with nonlinearities in the formulation. Under this assumption, the coupled governing equations are solved to obtain the temperature, stress and phase fields from four uncoupled problems: thermal, phase transformation, thermoelastic and elastoplastic. Classical numerical methods are applied to the uncoupled problems. Finite element method is employed for spatial discretization allowing the analysis of notched cylinders. Verification procedure treats numerical simulation of steel cylinders and results present good agreement with

those of experimental data obtained by the authors in previous works (Oliveira *et al.*, 2010). Afterwards, an investigation of stress concentration is carried out showing the influence of notches in steel cylinders.

2. CONSTITUTIVE MODEL

Constitutive equations may be formulated within the framework of continuum mechanics and the thermodynamics of irreversible processes, by considering thermodynamic forces, defined from the Helmholtz free energy, ψ , and thermodynamic fluxes, defined from the pseudo-potential of dissipation, ϕ (Pacheco *et al.*, 2001).

The proposed phenomenological quenching model allows one to identify different aspects related to quenching process. With this aim, a Helmholtz free energy is proposed as a function of observable variables, total strain, ε_{ij} , and temperature, T . Moreover, the following internal variables are considered: plastic strain, ε_{ij}^p , and volume fractions of seven different microstructures, represented by phases in a macroscopic point of view, $\beta = (\beta_0, \beta_1, \beta_2, \beta_3, \beta_4, \beta_5, \beta_6)$. A variable related to kinematic hardening, α_{ij} , is also considered. Therefore, the following free energy density is proposed, employing indicial notation where summation convention is evoked, except when indicated (Oliveira *et al.*, 2010):

$$\begin{aligned} \rho\psi(\varepsilon_{ij}, \varepsilon_{ij}^p, \alpha_{ij}, \varepsilon_{ij}^{tv}, \varepsilon_{ij}^{tp}, T, \beta_0, \beta_1, \beta_2, \beta_3, \beta_4, \beta_5, \beta_6) &= W(\varepsilon_{ij}, \varepsilon_{ij}^p, \alpha_{ij}, \varepsilon_{ij}^{tv}, \varepsilon_{ij}^{tp}, T, \beta_0, \beta_1, \beta_2, \beta_3, \beta_4, \beta_5, \beta_6) = \\ &= \sum_{m=0}^6 \beta_m W^{(m)}(\varepsilon_{ij}, \varepsilon_{ij}^p, \alpha_{ij}, \varepsilon_{ij}^{tv}, \varepsilon_{ij}^{tp}, T) + W_\beta(\beta_0, \beta_1, \beta_2, \beta_3, \beta_4, \beta_5, \beta_6) \end{aligned} \quad (1)$$

where ρ is the material density and $W_\beta(\beta_0, \beta_1, \beta_2, \beta_3, \beta_4, \beta_5, \beta_6) = J_\pi(\beta_0, \beta_1, \beta_2, \beta_3, \beta_4, \beta_5, \beta_6)$ represents the indicator function associated with the convex π

$$\pi = \{ \beta_m \in \mathfrak{R} \mid 0 \leq \beta_m \leq 1 \ (m = 0, 1, \dots, 6); \sum_{m=0}^6 \beta_m = 1 \} \quad (2)$$

The elastic strain can be written by assuming an additive decomposition:

$d\varepsilon_{ij}^e = d\varepsilon_{ij} - d\varepsilon_{ij}^p - \left(\sum_{m=0}^6 \beta_m \alpha_T^{(m)} \right) T \delta_{ij} - d\varepsilon_{ij}^{tv} - d\varepsilon_{ij}^{tp}$. In the right hand side of this expression, the first term is the total strain while the second is related to plastic strain. The third term is associated with thermal expansion. The parameter $\alpha_T^{(m)}$ is the coefficient of linear thermal expansion associated to phase m and δ_{ij} is the Kronecker delta. The fourth term is related to volumetric expansion associated with phase transformation from a parent phase $d\varepsilon_{ij}^{tv} = \left(\sum_{m=1}^6 \gamma_m d\beta_m \right) \delta_{ij}$, where γ_m is a material phase property related to total expansion. Finally, the last term is denoted as transformation plasticity strain $d\varepsilon_{ij}^{tp} = \sum_{m=1}^6 \frac{3}{2} \kappa_m f'(\beta_m) d\beta_m \sigma_{ij}^d$, being the result of several physical mechanisms related to local plastic strain promoted by the phase transformation (Denis *et al.*, 1985; Sjöström, 1985); κ_m is a material phase parameter, $f(\beta_m)$ expresses the transformation process dependence and σ_{ij}^d the deviatoric stress defined by $\sigma_{ij}^d = \sigma_{ij} - \delta_{ij} (\sigma_{kk}/3)$, with σ_{ij} being the stress tensor component. It should be emphasized that this strain may be related to stress states that are inside the yield surface.

In order to describe dissipation processes, it is necessary to introduce a potential of dissipation or its dual, which can be split into two parts $\phi^*(P_{ij}, Q_{ij}, R_{ij}, X_{ij}, B^\beta, g_i) = \phi_I^*(P_{ij}, Q_{ij}, R_{ij}, X_{ij}, B^\beta) + \phi_T^*(g_i)$. The set of constitutive equations is composed by the thermodynamics forces $(\sigma_{ij}, P_{ij}, Q_{ij}, R_{ij}, X_{ij}, T, B^\beta, g_i)$, associated with state variables $(\varepsilon_{ij}, \varepsilon_{ij}^p, \varepsilon_{ij}^{tv}, \varepsilon_{ij}^{tp}, \alpha_{ij}, s, \beta)$, and the thermodynamic fluxes are defined as follows:

$$\sigma_{ij} = \frac{\partial W}{\partial \varepsilon_{ij}} = \sum_{m=0}^6 \beta_m E_{ijkl}^{(m)} [\varepsilon_{kl} - \varepsilon_{kl}^p - \alpha_T^{(m)} (T - T_0) \delta_{kl} - \varepsilon_{kl}^{tv} - \varepsilon_{kl}^{tp}] \quad (3)$$

$$P_{ij} = -\frac{\partial W}{\partial \varepsilon_{ij}^p} = \sigma_{ij} \quad ; \quad Q_{ij} = -\frac{\partial W}{\partial \varepsilon_{ij}^{tv}} = \sigma_{ij} \quad ; \quad R_{ij} = -\frac{\partial W}{\partial \varepsilon_{ij}^{tp}} = \sigma_{ij} \quad ; \quad X_{ij} = -\frac{\partial W}{\partial \alpha_{ij}} = \left[\sum_{m=0}^6 \beta_m H_{ijkl}^{(m)} \right] \alpha_{kl} \quad (4)$$

$$s = -\frac{1}{\rho} \frac{\partial W}{\partial T} \quad ; \quad B^{\beta m} = -\frac{\partial W}{\partial \beta_m} \in -\partial_{\beta_m} J_\pi - \left[\frac{\partial W_e}{\partial \beta_m} + \frac{\partial W_\alpha}{\partial \beta_m} + \frac{\partial W_T}{\partial \beta_m} \right] \quad (m = 1, \dots, 6) \quad (5)$$

$$\dot{\varepsilon}_{ij}^p \in \partial_{P_{ij}} I_m^*(P_{ij}, X_{ij}) = \lambda \text{sign}[\sigma_{ij} - \left(\sum_{m=0}^6 \beta_r H_{ijkl}^{(m)} \right) \alpha_{kl}] \quad ; \quad \dot{\alpha}_{ij} \in -\partial_{X_{ij}} I_m^*(\sigma_{ij}, X_{ij}) = \dot{\varepsilon}_{ij}^p \quad (6)$$

$$\dot{\varepsilon}_{ij}^{tv} = \frac{\partial \phi^*}{\partial Q_{ij}} = \sum_{r=1}^6 \gamma^{(r)} \dot{\beta}_r \delta_{ij} \quad ; \quad \dot{\varepsilon}_{ij}^{tp} = \frac{\partial \phi^*}{\partial R_{ij}} = \sum_{m=1}^6 \frac{3}{2} \kappa^{(m)} f'(\beta_m) \dot{\beta}_m \sigma_{ij}^d \quad (7)$$

$$\dot{\beta}_M = \frac{\partial \phi^*}{\partial B^{\beta M}} = \zeta_{A \rightarrow M} \beta_A^0 [(1 - \beta_M) k T] \quad (8)$$

$$\dot{\beta}_m = \frac{\partial \phi^*}{\partial B \beta_m} = \zeta_{A \rightarrow m} \left\{ N_m(b_m)^{\left(\frac{1}{N_m}\right)} (\hat{\beta}_m^{max} - \beta_m) \left[\ln \left(\frac{\hat{\beta}_m^{max}}{\hat{\beta}_m^{max} - \beta_m} \right) \right]^{\left(1 - \frac{1}{N_m}\right)} \right\} \quad (m = 1, \dots, 5) \quad (9)$$

$$q_i = -\frac{\partial \phi^*}{\partial g_i} = -\left[\sum_{m=0}^6 \beta_m \Lambda^{(m)} \right] T g_i = -\left[\sum_{m=0}^6 \beta_m \Lambda^{(m)} \right] \frac{\partial T}{\partial x_i} \quad (10)$$

where $\partial_{\beta_r} J_{\pi}$ is the sub-differential of the indicator function J_{π} , $I_m^*(P_{ij}, X_{ij})$ is the indicator function associated with elastic domain, related to the *von Mises* criterion, λ is the plastic multiplier from the classical theory of plasticity (Lemaitre & Chaboche, 1990), $\text{sign}(x) = x / |x|$ and q_i is the heat flux vector. By assuming that the specific heat is $\left[\sum_{m=0}^6 \beta_m c^{(m)} \right] = -\left(\frac{T}{\rho} \right) \partial^2 W / \partial T^2$ and the set of constitutive equations (3-10), the energy equation can be written as (Pacheco, 1994):

$$\frac{\partial}{\partial x_i} \left(\left[\sum_{m=0}^6 \beta_r \Lambda^{(m)} \right] \frac{\partial T}{\partial x_i} \right) - \rho \left[\sum_{m=0}^6 \beta_m c^{(m)} \right] \dot{T} = -a_I - a_T \quad (11)$$

where:

$$\begin{cases} a_I = \sum_{m=1}^6 B \beta_m \dot{\beta}_m - X_{ij} \dot{\epsilon}_{ij}^p + \sigma_{ij} (\dot{\epsilon}_{ij}^p + \dot{\epsilon}_{ij}^{tv} + \dot{\epsilon}_{ij}^{tp}) \\ a_T = T \left[\frac{\partial \sigma_{ij}}{\partial T} (\dot{\epsilon}_{ij} - \dot{\epsilon}_{ij}^p - \dot{\epsilon}_{ij}^{tv} - \dot{\epsilon}_{ij}^{tp}) - \sum_{m=1}^6 \frac{\partial B \beta_m}{\partial T} \dot{\beta}_m + \frac{\partial X_{ij}}{\partial T} \dot{\epsilon}_{ij}^p \right] \end{cases} \quad (12)$$

Terms a_I and a_T are, respectively, internal and thermal coupling. The thermomechanical coupling effect related to phase transformation may be represented as a latent heat released during the phase transformation (Fernandes *et al.*, 1985; Denis *et al.*, 1987; Woodard *et al.*, 1999):

$$a_I + a_T = \dot{Q} = \sum_{m=1}^6 \Delta H_m \dot{\beta}_m \quad (13)$$

where ΔH_m is the enthalpy variation in a transformation process involving a previous phase (austenite) and a product phase β_m ($m = 1, \dots, 6$). Therefore, this source term is used instead of all thermomechanical couplings effects, which represents a first approach of the general formulation (Silva *et al.*, 2004).

This contribution considers cylindrical bodies as an application of the proposed general formulation. An axisymmetric finite element model is developed to study the quenching process in cylinders. The numerical procedure here proposed is based on the operator split technique (Ortiz *et al.*, 1983; Pacheco, 1994) associated with an iterative numerical scheme in order to deal with nonlinearities in the formulation. With this assumption, coupled governing equations are solved from four uncoupled problems: thermal, phase transformation, thermo-elastic and elastoplastic.

Thermal Problem - Comprises a conduction problem with convection and radiation. Material properties depend on temperature, and therefore, the problem is governed by non-linear parabolic equations. Finite element method is used for numerical solution.

Phase Transformation Problem - The volume fractions of the phases are determined in this problem. Evolution equations are integrated from a simple implicit Euler method.

Thermo-elastic Problem - Stress and displacement fields are evaluated from temperature distribution. Numerical solution is obtained employing the finite element method.

Elastoplastic Problem - Stress and strain fields are determined considering the plastic strain evolution in the process. Numerical solution is based on the classical return mapping algorithm (Simo & Hughes, 1998).

A detailed description of the model could be found in Pacheco *et al.* (2001), Silva *et al.* (2004, 2005) and Oliveira (2008).

3. ANALYSIS OF A STEEL CYLINDER

The forthcoming analysis promotes a verification of the proposed model establishing a comparison with experimental data obtained in Oliveira *et al.* (2010). Besides model verification, this section also presents an analysis of stress evolution during the process. An SAE 4140H, 25.4mm (1") radius cylinder quenched in air and water are considered. Material parameters of the SAE 4140H are the following (Denis *et al.*, 1985, 1999; Woodard, *et al.*, 1999; Sjöström, 1985; Melander, 1985; Oliveira, 2004): $\gamma_1 = 3.333 \times 10^{-3}$, $\gamma_2 = 0$, $\gamma_3 = \gamma_4 = \gamma_5 = 5.000 \times 10^{-3}$, $\gamma_6 = 1.110 \times 10^{-2}$, $\kappa_m = \left[5 / (2 \sigma_Y^o) \right] \gamma_m$ (where σ_Y^o is the austenite yielding stress and $m=1, \dots, 6$), $\rho = 7.800 \times 10^3 \text{ kg/m}^3$, $M_s = 340^\circ\text{C}$, $M_f = 140^\circ\text{C}$. Other parameters depend on temperature and needs to be interpolated from experimental data. Therefore, parameters $E^m, H^m, \sigma_Y^m, \alpha_T^m, c^m, \Lambda^m$ ($m=1, \dots, 6$) and the convection coefficient, h , are evaluated by polynomial expressions (Melander, 1985; Hildenwall, 1979; Pacheco *et al.*, 2001; Silva *et al.*, 2004; Oliveira *et al.*,

2010). Temperature dependent parameters for diffusive phase transformations are obtained from TTT diagrams (ASM, 1977). Moreover, latent heat released associated with the enthalpy variation in a transformation process involving a parent phase (austenite) and a product phase β_m are given by: $\Delta H_1 = 1.55 \times 10^9 - 2.31 \times 10^6 T + 1597 T^2 - 0.429 T^3 - 5.00 \times 10^{11} / T \text{ J/m}^3$, $\Delta H_3 = \Delta H_4 = \Delta H_5 = 1.56 \times 10^9 - 1.5 \times 10^6 T \text{ J/m}^3$, $\Delta H_6 = 640 \times 10^6 \text{ J/m}^3$ (Denis *et al.*, 1987; Woodard *et al.*, 1999; Stull & Prophet, 1971).

Finite element analysis is performed exploiting a single strip axisymmetrical geometry for simulations. For long cylinders subjected to through hardening, far from the ends, the process along the cylinder is similar and the analysis can be performed in a thin strip. Figure 1 shows the axisymmetric finite element model mesh obtained after a convergence analysis where z is axisymmetry axis. Mechanical and thermal boundary conditions are associated with plane stress condition: prescribed z -direction null displacement at $z = 0$ (symmetry condition); prescribed z -direction null heat flux at $z = 0$ and $z = h$; convection and radiation at external surface. In all simulations developed τ_{rz} presents small values in the whole piece.

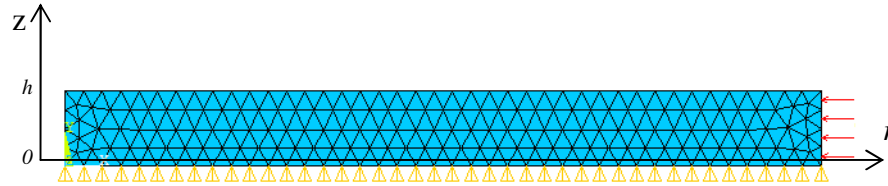


Figure 1. Finite element mesh and boundary conditions.

3.1. Model Verification

Initially, air cooling is of concern. In order to compare numerical and experimental results, Figures 2a and 2b presents the temperature time history in two different positions: at the center and at 1 mm from the surface of the cylinder. It is noticeable the close agreement between results and it is important to highlight that the thermomechanical coupling effect is captured by the model. As expected, the model shows the temperature increase at about 650°C, which is associated with the latent heat of the austenite → pearlite phase transformation. In terms of volume fraction distribution, model predicts 27% of ferrite and 73% of pearlite that is in close agreement with experimental results, as presented in Figure 2c.

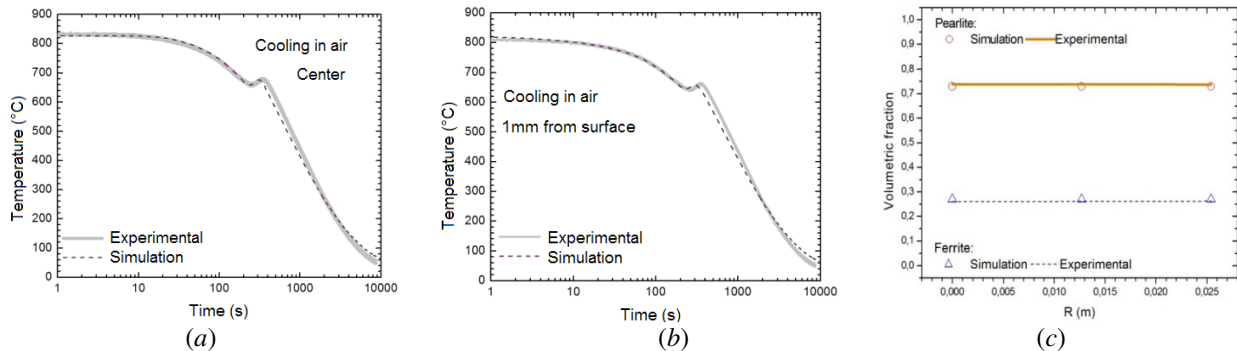


Figure 2. Air cooling temperature time history: (a) at the center and (b) at 1 mm from the cylinder surface. Phase distribution along the cylinder radius (c).

The quenching process in water is now in focus. Temperature time history in two different positions (at the center of the cylinder and at 1 mm from the cylinder surface) is presented in Figures 3a and 3b. At the body center there is a close agreement between numerical and experimental results. By considering the position at 1mm from the surface, on the other hand, results capture just the general behavior. This discrepancy is explained by the thermocouple influence. Actually, it is possible to make adjustments considering the heat conduction through the thermocouple and evaluating the temperature at its center. In terms of volume fraction distribution the model predicts 100% of martensite at the surface and 91% at the center of the cylinder. This implies an amount of 9% of bainite that is a small difference when compared to experimental data. Nevertheless, it is important to observe that experimental data uses optical analysis in order to conclude the phase distribution and therefore, this difference may be less than presented. The Figure 3c shows the phase distribution along the cylinder radius.

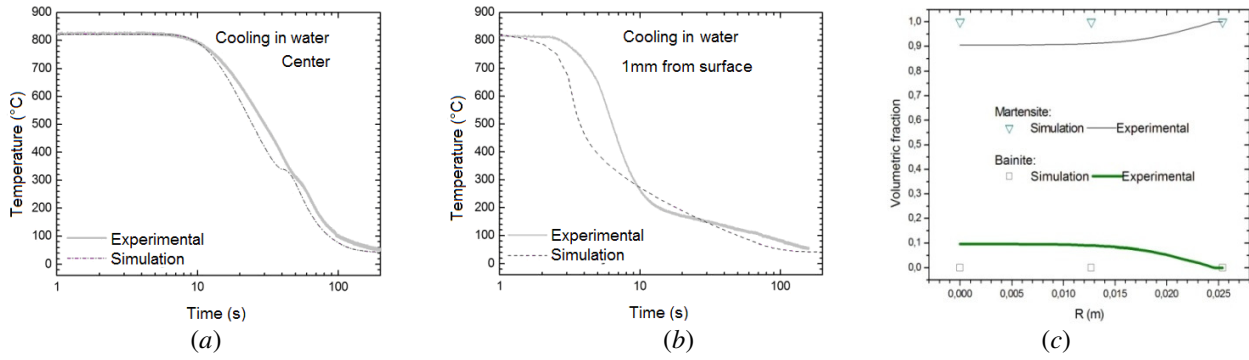


Figure 3. Air cooling temperature time history: (a) at the center and (b) at 1 mm from the surface for the cylinders. Phase distribution along the cylinder radius (c).

3.2. Stresses Analysis

Stress time evolution present a very complex behavior associated with the coupling between the different phenomena involved. The behavior of the stress field during the quenching process is now in focus. Figures 4 and 5 present, respectively, for air and water cooling the stress time evolution (σ_r, σ_θ and σ_z) for five different positions: $r = 0$; $r = 1/4R$; $r=1/2R$; $r = 3/4R$; $r=R$. Basically, the stress time evolution can be understood by considering three main stages: start cooling, phase transformation and end cooling.

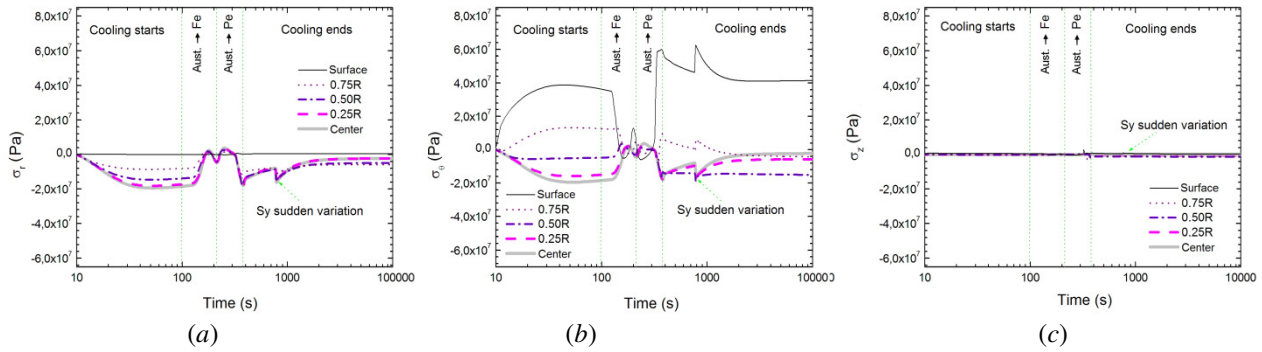


Figure 4- Stress time evolution: (a) σ_r , (b) σ_θ and (c) σ_z . Air cooling.

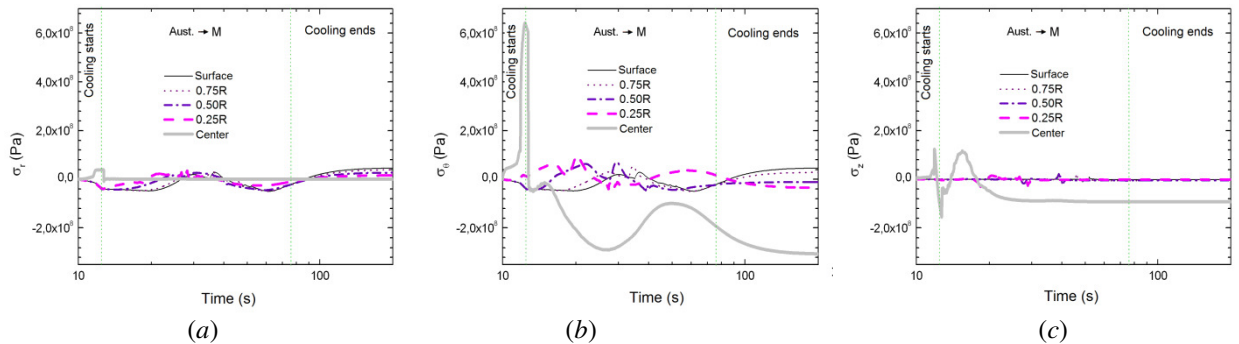


Figure 5. Stress distribution during the time, at plane stress: (a) σ_r , (b) σ_θ and (c) σ_z . Water cooling.

Convection and radiation phenomena induce faster cooling at the cylinder surface promoting a contraction of this region in contrast of the expansion at the center of the cylinder. The phase transformation process has an important influence in stress distribution during quenching process. There is a competition between phase transformation effects and thermal effects. At the beginning of the phase transformation, these effects are more important but, at the end of these transformations, thermal effects become more relevant. Component τ_{rz} has low values during all the process and, therefore, is neglected in the analysis.

The use of water as a cooling medium makes quenching a severe process to the specimen. Under this condition, the mechanical behavior observed at the cylinder surface is more intense than other regions of the cylinder. Transformation plasticity plays an important role in this process changing the residual stress distribution. Figure 6 shows the residual stress distribution for the air and water cooling media at the end of the quenching process when temperatures tend to be

homogeneous in the whole piece and it is possible to identify permanent strains in the specimen. Water cooling presents large values when compared with air cooling.

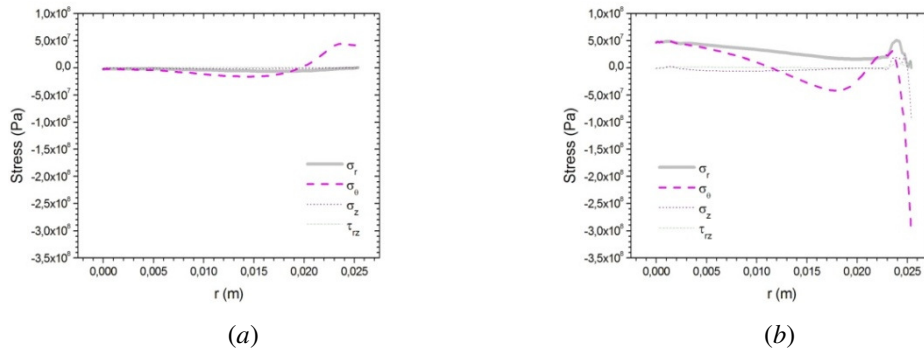


Figure 6. Stress distribution at the end of the process: (a) air and (b) water cooling.

4. ANALYSIS OF STRESS CONCENTRATION

This section presents an analysis of stress concentration in steel cylindrical bodies subjected to quenching. Essentially, the influence of stress concentration is verified evaluating residual stress distribution that occurs during the quenching process. Cylindrical bodies with radius of 25.4 mm and height of 15.24 mm are treated with stress concentration promoted by circular radius that varies from 0.00 mm to 5.08 mm.

Since water is related to a more severe quenching condition, water is assumed as a cooling medium. Moreover, mechanical boundary conditions are assumed to be in such a way that constrains the displacement at the top and the bottom surface of the cylinder, as presented in Figure 7a. Different geometrical configurations are treated as shown in Figures 7b-7f. Basically, notches with five radius are considered assuming different values of the ratio r/R : 0, 0.05, 0.10, 0.15, 0.20. Finite element discretization is defined by meshes chosen from a convergence analysis that takes into account time and space discretization.

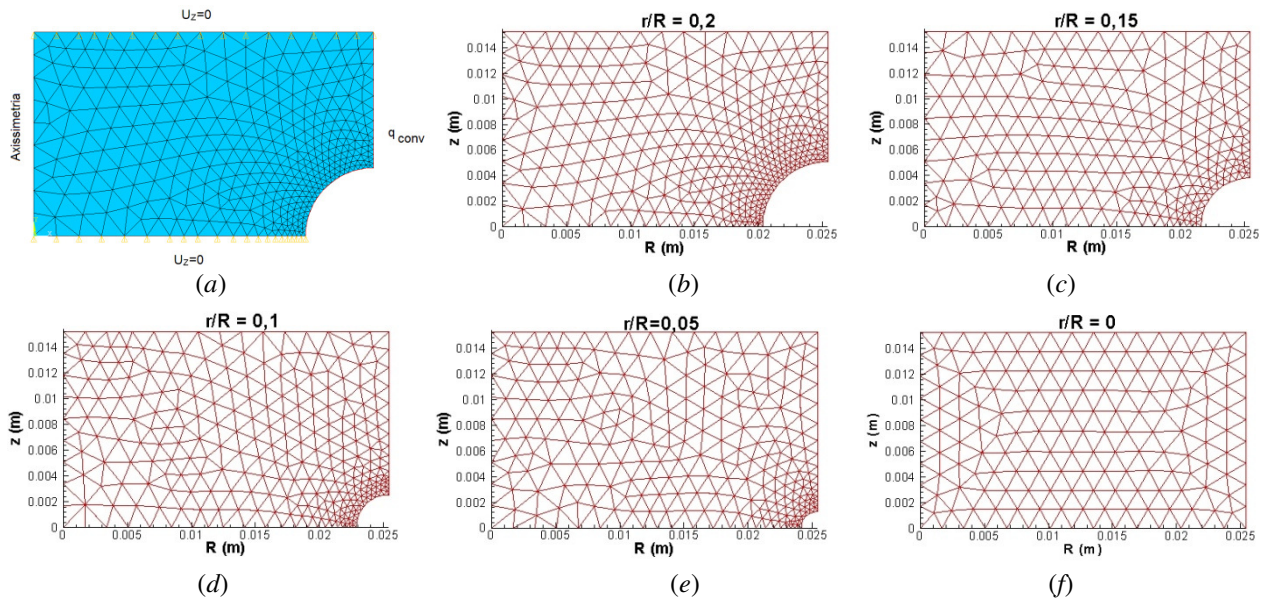


Figure 7. Boundary conditions: geometries with stress concentrators (a). Meshes adopted in simulations: (b) $r/R=0,20$; (c) $r/R=0,15$; (d) $r/R=0,10$; (e) $r/R=0,05$; (f) $r/R=0$.

Initially, phase transformation is investigated showing phases distribution at the end of the quenching process for each one of the different geometries. Figure 8 presents the martensite volume fraction distribution showing that the stress concentration tends to induce phase transformation. Note that martensite is the predominant phase, with minimal volume fraction of 0.91 at cylinder center and maximum volumetric fraction of 1 at cylinder surface. The bainite volume fraction is given by $(1-\beta_M)$.

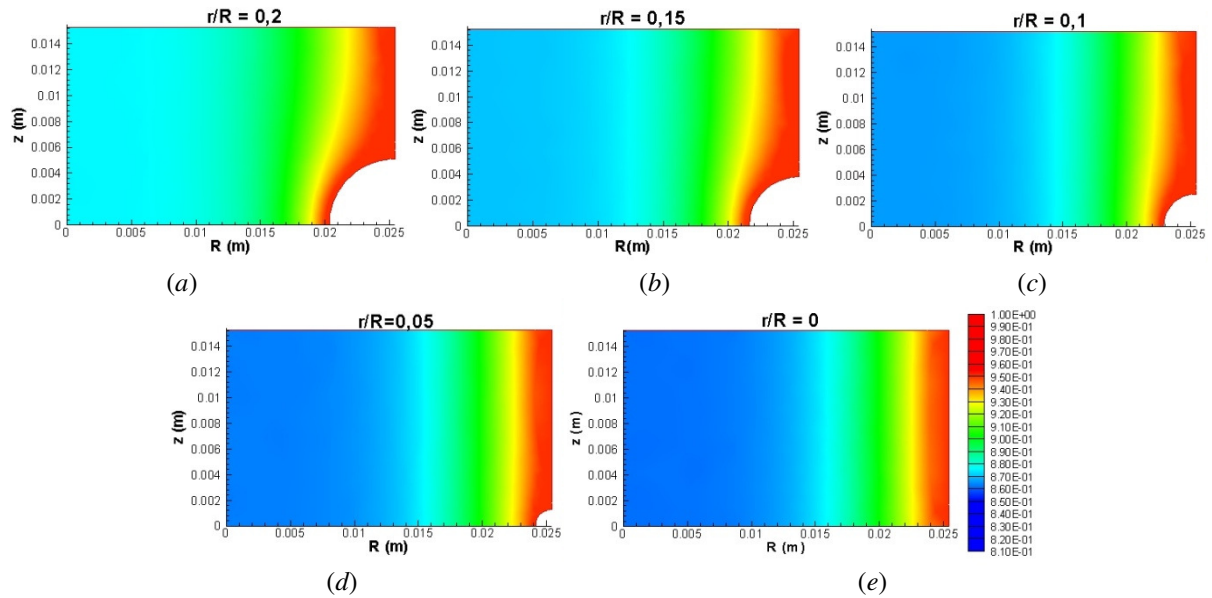


Figure 8. Martensite volume fraction distribution: (a) $r/R=0,20$; (b) $r/R=0,15$; (c) $r/R=0,10$; (d) $r/R=0,05$; (e) $r/R=0$.

A discussion about the residual stress distribution at the end of the quenching process is now in focus. Figure 9 presents the distribution of σ_r stress at the last time instant. The higher tensile stress occurs around the stress concentrator, while the higher compression values are observed in a region close to the center of the bodies. Figure 13a summarizes higher tensile and compressive stresses for all geometries. It should be highlighted that the higher tensile stress occurs at the piece with stress concentrator $r/R = 0.10$ and the higher compressive stress occurs at the piece with stress concentrator $r/R = 0.20$

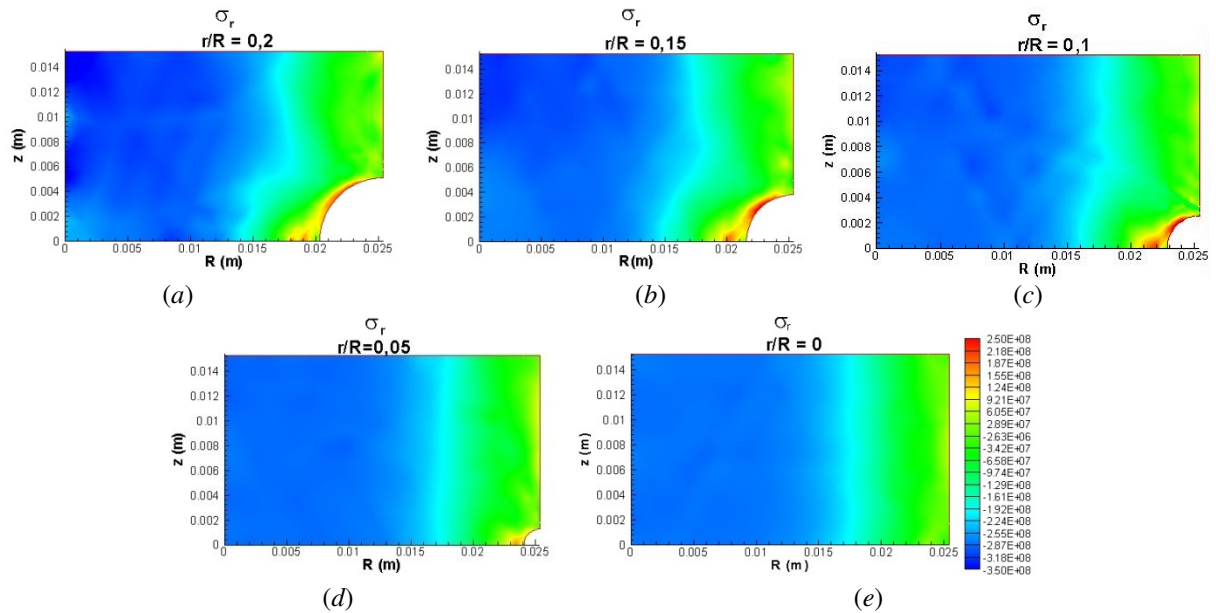


Figure 9. σ_r (Pa): (a) $r/R=0.20$; (b) $r/R=0.15$; (c) $r/R=0.10$; (d) $r/R=0.05$; (e) $r/R = 0$.

An analysis of σ_θ stress component is now in focus. Figure 10 presents the stress distribution that shows that the higher tensile stress occurs near the stress concentrator (about 0.5 mm far), while the higher compression values are observed in a region close to the center of the cylinder. Figure 13b summarizes higher tensile and compressive stresses showing that stress concentrator $r/R = 0.20$ presents higher tensile stresses and the higher compressive stress occurs at the piece with stress concentrator $r/R = 0.15$.

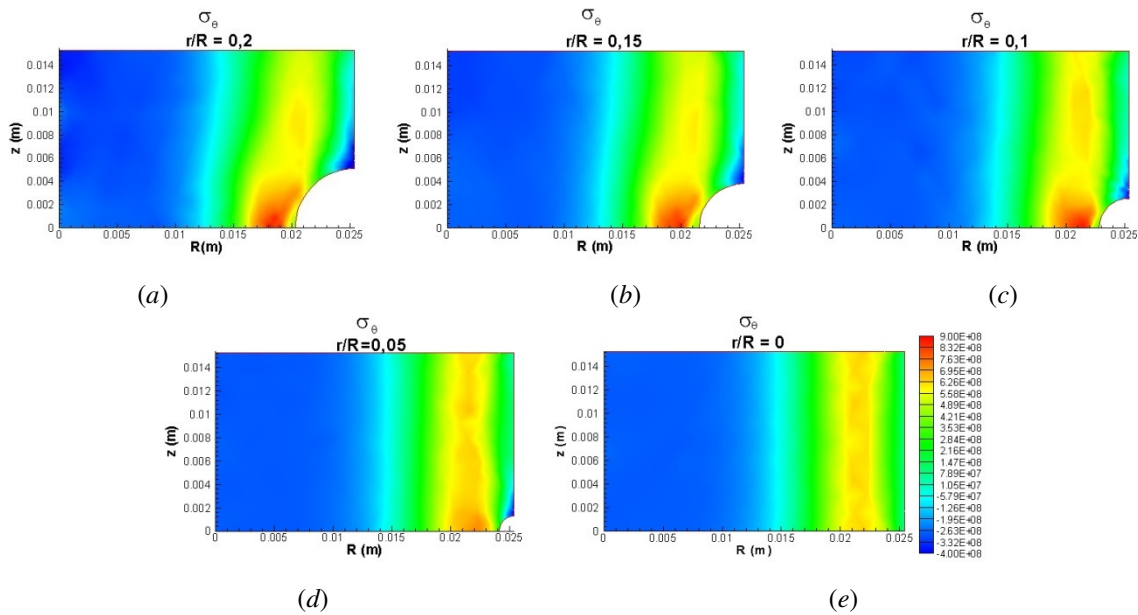


Figure 10. σ_θ (Pa): (a) $r/R=0.20$; (b) $r/R=0.15$; (c) $r/R=0.10$; (d) $r/R=0.05$; (e) $r/R = 0$.

Stress σ_z distribution is now focused on, as shown in Figure 11. The higher tensile stress occurs in the deep region of the stress concentrator and the higher compression values are observed in a region close to the center of the cylinder. It is important to mention that in the piece with $r/R = 0.20$, a relevant compressive region at surface is observed. Figure 13c presents a summary of higher tensile and compressive stresses that shows that the higher tensile stress occurs at the piece with stress concentrator $r/R = 0.10$ while the higher compressive stress occurs at the piece with stress concentrator $r/R = 0.20$.

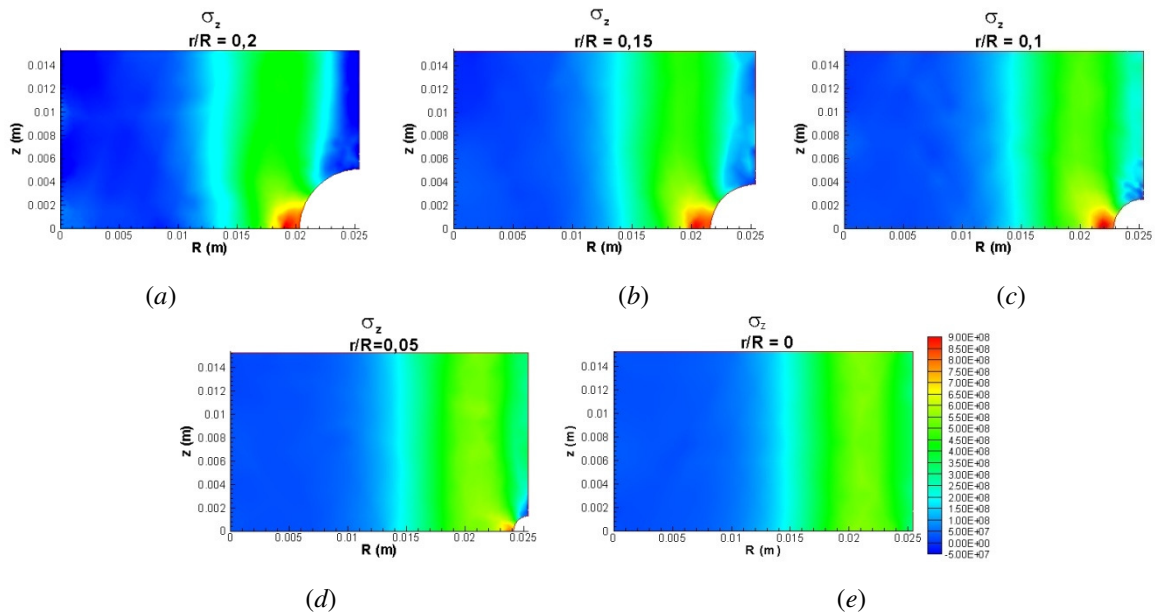


Figure 11. σ_z (Pa): (a) $r/R=0.20$; (b) $r/R=0.15$; (c) $r/R=0.10$; (d) $r/R=0.05$; (e) $r/R = 0$.

An alternative to observe stress analysis is the *von Mises* stress distribution. Figure 12 presents this equivalent stress distribution for five different geometries. The higher stress occurs in a region close to the stress concentrator. Figure 13d summarizes these results presenting higher stress values. The presented results show that the *von Mises* stress, at the high stress region, has a direct relation to stress concentrator radius, however, the difference between the higher stress of the piece with stress concentrator $r/R = 0.15$ and the higher stress of the piece without stress concentrator is equal to 64 MPa. This leads that stress concentration presents a low influence in residual *von Mises* stresses.

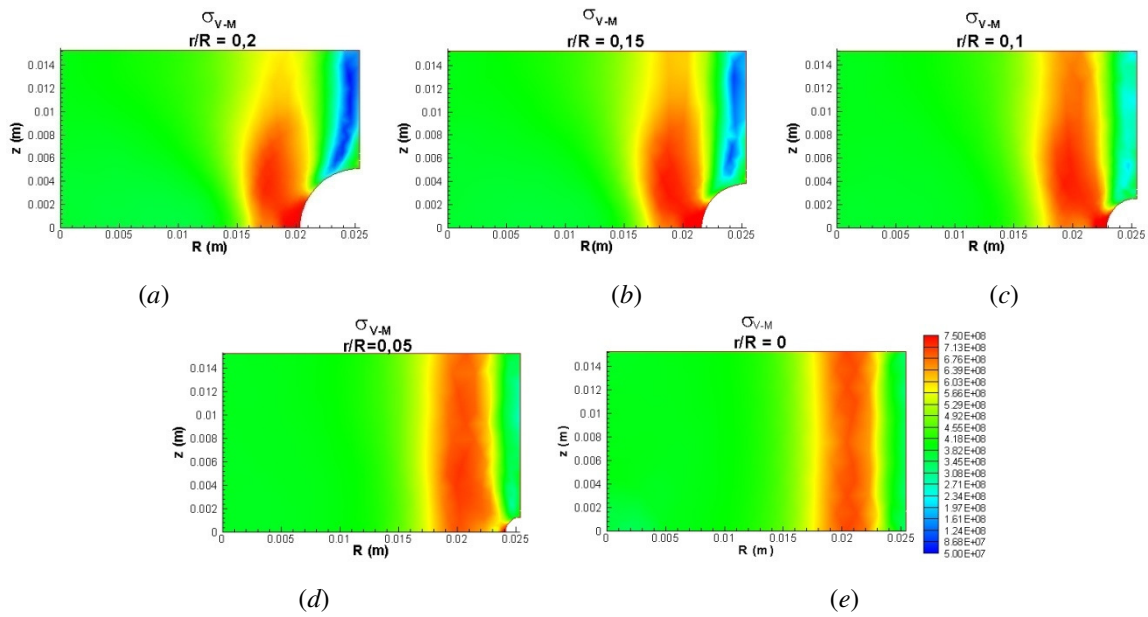


Figure 12. σ_{von_Mises} (Pa): (a) $r/R=0.20$; (b) $r/R=0.15$; (c) $r/R=0.10$; (d) $r/R=0.05$; (e) $r/R = 0$.

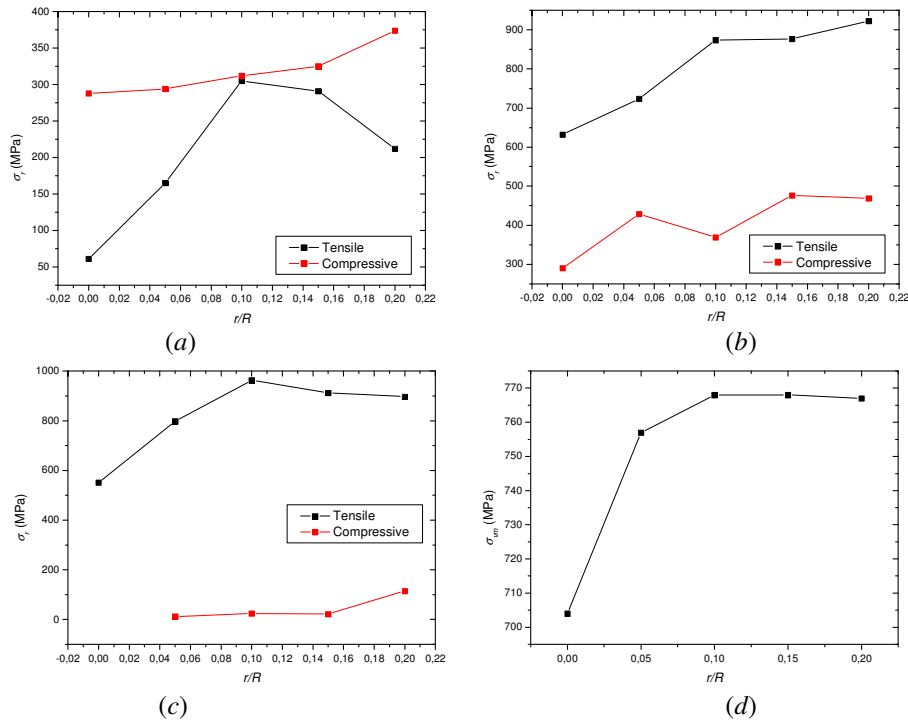


Figure 13. Maximum stresses, of cylinders with stress concentrators: (a) σ_r , (b) σ_θ , (c) σ_z , (d) $\sigma_{vonMises}$.

5. CONCLUSIONS

This contribution deals with modeling and simulation of quenching process, presenting an anisothermal multi-phase constitutive model formulated within the framework of continuum mechanics and thermodynamics of irreversible processes. This approach allows a direct extension to more complex situations, as the analysis of three-dimensional media. A numerical procedure is developed based on the operator split technique associated with an iterative numerical scheme in order to deal with nonlinearities in the formulation. The proposed numerical procedure allows the use of traditional numerical methods, like the finite element method. Through hardening of cylindrical bodies is considered as application of the proposed general formulation. Numerical results establishes a model verification using experimental data as a reference. Besides, notched steel cylinder are of concern evaluating the influence of notches during quenching process. In general, it is possible to say that the proposed model is capable of capturing the general behavior quenching and, therefore, it can be used as a tool to predict the thermomechanical behavior of quenched mechanical components. Important parameters as the cooling medium and the induced layer thickness are some possibilities to be analyzed by the proposed procedure.

6. ACKNOWLEDGEMENTS

The authors would like to acknowledge the support of the Brazilian Research Agencies CNPq and FAPERJ and through the INCT-EIE (National Institute of Science and Technology - Smart Structures in Engineering) the CNPq and FAPEMIG. The Air Force Office of Scientific Research (AFOSR) is also acknowledged.

7. REFERENCES

- ASM, 1977, “*Atlas of Isothermal Transformation and Cooling Transformation Diagrams*”, American Society Metals.
- Çetinel, H., Toparlı, M. & Özsoyler, 2000, “A Finite Element Based Prediction of the Microstructural Evolution of Steels Subjected to the Tempcore Process”, *Mechanics of Materials*, v.32, pp.339-347.
- Chen, J. R., Tao, Y. Q. & Wang, H.G., 1997, “A Study on Heat Conduction with Variable Phase Transformation Composition during Quench Hardening”, *Journal of Materials Processing Technology*, v.63, pp.554-558.
- Denis, S., Gautier, E., Simon, A. & Beck, G., 1985, “Stress-Phase-Transformation Interactions – Basic Principles, Modelling and Calculation of Internal Stresses”, *Material Science and Technology*, v.1, October, p.805-814.
- Denis, S., Sjöström, S. & Simon, A., 1987, “Coupled Temperature, Stress, Phase Transformation Calculation Model Numerical Illustration of the Internal Stresses Evolution during Cooling of a Eutectoid Carbon Steel Cylinder”, *Metallurgical Transactions A*, v.18A, July, pp.1203-1212.
- Denis, S., Archambault, S., Aubry, C., Mey, A., Louin, J. C. & Simon, A., 1999, “Modelling of Phase Transformation Kinetics in Steels and Coupling with Heat Treatment Residual Stress Predictions”, *J. de Phys. IV*, v.9, pp.323-332.
- Fernandes, M.B., Denis, S. & Simon, A., 1985, “Mathematical Model Coupling Phase Transformation and Temperature Evolution during Quenching of Steels”, *Materials Science and Technology*, v.1, October, pp.838-844.
- Hildenwall, B., 1979, “*Prediction of the Residual Stresses Created During Quenching*”, Ph.D. Thesis, Linköping Univ.
- Hömberg, D., 1996, “A Numerical Simulation of the Jominy End-quench Test”, *Acta Mater.*, v.44, n.11, pp.4375-4385
- Inoue, T. & Wang, Z., 1985, “Coupling between Stress, Temperature, and Metallic Structures during Processes Involving Phase Transformations”, *Material Science and Technology*, v.1, pp.845-850.
- Lemaitre, J. & Chaboche, J.L., 1990, “*Mechanics of Solid Materials*”, Cambridge Press Univ.
- Melander, M., 1985, “*A Computational and Experimental Investigation of Induction and Laser Hardening*”, Ph.D. Thesis, Department of Mechanical Eng., Linköping University.
- Ortiz, M., Pinsky, P. M. & Taylor, R. L., 1983, “Operator Split Methods for the Numerical Solution of the Elastoplastic Dynamic Problem”, *Computer Methods in Applied Mechanics and Engineering*, v.39, pp.137-157.
- Oliveira, W. P., 2004, “*Modeling Quenching Process in Steel Cylinder Using Multi-Phase Constitutive Model*”, M.Sc. Dissertation, CEFET/RJ, in Portuguese.
- Oliveira, W. P., 2008, “*Modeling and Simulation of Quenching in Axisymmetrical Geometries Using a Multi-Phase Constitutive Model*”, Ph.D. Thesis, COPPE/UFRJ, in Portuguese.
- Oliveira, W. P., Savi, M. A., Pacheco, P. M. C. L. & Souza, L. F. G., 2010, “Thermomechanical Analysis of Steel Cylinders Quenching Using a Constitutive Model with Diffusional and Non-Diffusional Phase Transformations”, *Mechanics of Materials*, v.42, n.1, pp.31-43.
- Pacheco, P. M. C. L., 1994, “*Analysis of Thermomechanical Coupling in Elasto-viscous-plastic Materials*”, Ph.D. Thesis, Department of Mechanical Engineering, PUC-Rio.
- Pacheco, P. M. C. L., Savi, M. A. & Camarão, A. F., 2001, “Analysis of Residual Stresses Generated by Progressive Induction Hardening of Steel Cylinders”, *Journal of Strain Analysis for Engineering Design*, v.36, n.5, pp.507-516.
- Reti, T., Fried, Z. & Felde, I., 2001, “Computer Simulation of Steel Quenching Process using a Multi-Phase Transformation Model”, *Computational Materials Science*, v.22, pp.261-278.
- Sen, S., Aksakal, B. & Ozel, A., 2000, “Transient and Residual Thermal Stresses in Quenched Cylindrical Bodies”, *International Journal of Mechanical Sciences*, v.42 n.10, p.2013-2029.
- Silva, E. P., Pacheco, P. M. C. L. & Savi, M. A., 2004, “On the Thermo-Mechanical Coupling in Austenite-Martensite Phase Transformation Related to the Quenching Process”, *Int. J. of Solids and Struct.*, v.41, n.3-4, pp.1139-1155.
- Silva, E. P., Pacheco, P. M. C. L. & Savi, M. A., 2005, “Finite Element Analysis of the Phase Transformation Effect in Residual Stresses Generated by Quenching in Notched Steel Cylinders”, *Journal of Strain Analysis for Engineering Design*, v.40, n.2, p.151-160.
- Simo, J. C. & Hughes, T. J. R., 1998, “*Computational Inelasticity*”, Springer.
- Sjöström, S., 1985, “Interactions and Constitutive Models for Calculating Quench Stresses in Steel”, *Material Science and Technology*, v.1, p.823-829.
- Stull, D. R. & Prophet, H., 1971, “*Janaf Thermochemical Tables*”, National Standard Ref. Data System, 2 Ed. NBS 37.
- Woodard, P. R., Chandrasekar, S. & Yang, H. T. Y., 1999, “Analysis of Temperature and Microstructure in the Quenching of Steel Cylinders”, *Metallurgical and Materials Trans.*

8. RESPONSIBILITY NOTICE

The authors are the only responsible for the printed material included in this paper.